6146 *Chem. Mater.* **2010,** *22,* 6146–6152
DOI:10.1021/cm1019684

CHEMISTRY OF MATERIALS
Article

Resorcinol-Based Deep Eutectic Solvents as Both Carbonaceous Precursors and Templating Agents in the Synthesis of Hierarchical Porous Carbon Monoliths

Daniel Carriazo, María C. Gutiérrez,* M. Luisa Ferrer, and Francisco del Monte*

Instituto de Ciencia de Materiales de Madrid (ICMM), Consejo Superior de Investigaciones Científicas (CSIC), Campus de Cantoblanco, 28049 Madrid, Spain

Received July 15, 2010. Revised Manuscript Received September 7, 2010

Deep eutectic solvents are a new class of ionic liquids obtained via the complexion of quaternary ammonium salts with hydrogen-bond donors (such as acids, amines, and alcohols, among others). The charge delocalization that occurs through hydrogen bonding between the halide anion with the hydrogen-donor moiety is responsible for the decrease in the freezing point of the mixture, relative to the melting points of the individual components. We have recently reported on the use of deep eutectic solvents as suitable solvents, to carry out the polycondensation of resorcinol−formaldehyde. [*Chem. Mater.* **2010**, *22*, 2711−2719.] Herein, we describe the synthesis of deep eutectic solvents (DESs) based on resorcinol, the use of which as both carbonaceous precursors and structure-directing agents allowed the preparation of hierarchical porous (bimodal, with micropores and mesopores) carbon monoliths via formaldehyde polycondensation and subsequent carbonization. The performance of resorcinol-based DESs as carbonaceous precursors was remarkable, with carbon conversions of ∼80%. Moreover, the use of DESs as structure-directing agents resulted in the achievement of hierarchical porous carbon monoliths with pore surface areas up to 600 m^2/g and narrow mesopore diameter distributions. The mechanism governing the formation of mesopores was based on a spinodal-decomposition-like-process via resorcinol polycondensation and subsequent segregation of the resorcinol counterpart that is forming the DESs. Thus, the use of resorcinol-based DESs that have different counterparts (e.g., either choline chloride or a mixture of choline chloride and urea) allowed the preparation of hierarchical carbons with tailored mesopore diameters of ca. 23 nm and ca. 10 nm.

Introduction

Carbon materials exhibiting three-dimensional (3D) hierarchical porous textures (combining pores at different scales, from macropores to mesopores, up to micropores) are outstanding candidates for many applications, ranging from water and air purification, adsorption, or catalysis, to electrodes and energy storage, because of their high surface area, large pore volume, chemical inertness, and excellent mechanical stability.[1,2]

Both hard and soft template methods have been used to reach such porous carbonaceous materials. The hard-template methodology (first reported in the works of Ryoo[3] and Hyeon[4]) makes use of preformatted, hard, porous templates impregnated with a carbon source that is subsequently carbonized under a nonoxidative atmosphere.[5] After dissolution of the hard template, a negative, carbonaceous replica is finally obtained. More recently, highly ordered and well-oriented mesoporous carbons have been obtained through the use of block copolymers (e.g., PS-P4VP, F127, P123, etc.) as soft templates, typically using resorcinol as carbon sources.[6] The capability of some of these latter approaches (either by themselves[6e,6f,6g] or in combination with hard templates[7]) to process 3D hierarchical porous carbons in form of monoliths (easy to handle and capable of being directly assembled into a

*Author to whom correspondence should be addressed. E-mails: mcgutierrez@icmm.csic.es, delmonte@icmm.csic.es.

(1) Al-Muhtaseb, S. A.; Ritter, J. A. *Adv. Mater.* **2003**, *15*, 101–114.
(2) (a) Fan, L. Z.; Hu, Y. S.; Maier, J.; Adelhelm, P.; Smarsly, B.; Antonietti, M. *Adv. Funct. Mater.* **2007**, *17*, 3083–3087. (b) Xia, Y.; Mokaya, R. *J. Phys. Chem. C* **2007**, *111*, 10035–10039. (c) Yang, H. F.; Shi, Q. H.; Liu, X. Y.; Xie, S. H.; Jiang, D. C.; Zhang, F. Q.; Yu, C. Z.; Tu, B.; Zhao, D. Y. *Chem. Commun.* **2002**, 2842–2843. (d) Wang, D.-W.; Li, F.; Liu, M.; Lu, G. Q.; Cheng, H.-M. *Angew. Chem., Int. Ed.* **2008**, *47*, 373–376. (e) Lu, A. H.; Schüth, F. *Chem. Mater.* **2008**, *20*, 5314–5319.
(3) Joo, S. H.; Choi, S. J.; Oh, I.; Kwak, J.; Liu, Z.; Terasaki, O.; Ryoo, R. *Nature* **2001**, *412*, 169.
(4) Lee, J.; Yoon, S.; Hyeon, T.; Oh, S. M.; Kim, K. B. *Chem. Commun.* **1999**, 2177.
(5) (a) Schüth, F. *Angew. Chem., Int. Ed.* **2003**, *42*, 3604. (b) Woo, S.-W.; Dokko, K.; Nakano, H.; Kanamura, K. *J. Mater. Chem.* **2008**, *18*, 1674–1680.
(6) (a) Liang, C.; Hong, K.; Guiochon, G. A.; Mays, J. W.; Dai, S. *Angew. Chem., Int. Ed.* **2004**, *43*, 5785. (b) Tanaka, S.; Nishiyama, N.; Egashira, Y.; Ueyama, K. *Chem. Commun.* **2005**, 2125. (c) Liu, C.; Li, X.; Song, H.; Chen, X. *Chem. Commun.* **2007**, 757. (d) Meng, Y.; Gu, D.; Zhang, F.; Shi, Y.; Yang, H.; Li, Z.; Yu, C.; Tu, B.; Zhao, D. *Angew. Chem., Int. Ed.* **2005**, *44*, 7053. (e) Huang, Y.; Cai, H.; Feng, D.; Gu, D.; Deng, Y.; Tu, B.; Wang, H.; Webley, P. A.; Zhao, D. *Chem. Commun.* **2008**, 2641–2643. (f) Gutierrez, M. C.; Pico, F.; Rubio, F.; Amarilla, M.; Palomares, F. J.; Ferrer, M. L.; del Monte, F.; Rojo, J. M. *J. Mater. Chem.* **2009**, *19*, 1263–1240. (g) Carriazo, D.; Pico, F.; Gutierrez, M. C.; Rubio, F.; Rojo, J. M.; del Monte, F. *J. Mater. Chem.* **2010**, *20*, 773–780. (h) Valkama, S.; Nykänen, A.; Kosonen, H.; Ramani, R.; Tuomisto, F.; Engelhardt, P.; ten Brinke, G.; Ikkala, O.; Ruokolainen, J. *Adv. Funct. Mater.* **2007**, *17*, 183–190.

 Published on Web 10/28/2010

particular device) offer additional advantages for practical applications.

Recently, ionic liquids (ILs)[8] and deep eutectic solvents (DESs)[9] have been the solvent of choice in several chemical reactions, because of their special features; e.g., they are nonreactive with water, nonvolatile, and biodegradable. DESs are a new class of IL; they are obtained via the complexion of quaternary ammonium salts with hydrogen-bond donors (such as acids, amines, and alcohols, among others).[10] The charge delocalization that occurs through hydrogen bonding between the halide anion with the hydrogen-donor moiety is responsible for the decrease of the freezing point of the mixture, relative to the melting points of the individual components. ILs and DESs have been used as templates for the preparation of zeolites,[11] metal−organic frameworks,[12,13] and inorganic−organic hybrids.[14] The preparation of carbonaceous materials has also been described using ILs and DESs as solvents[15] and even as carbonaceous precursors.[16] However, the capability of DESs to template the structure of the resulting carbon has never been explored.

Herein, we describe the use of DESs based on resorcinol complexes as both carbonaceous precursors (via formaldehyde polycondensation and subsequent carbonization) and structure-directing agents for preparation of carbon monoliths exhibiting a hierarchical porous structure. The DESs of choice were based on two different complexes of resorcinol: one binary with choline chloride, called RC1-DES and RC2-DES (depending on resorcinol:choline chloride molar ratio used for preparation (4:1 and 3.75:1, respectively)), and the other ternary with urea and choline chloride, called RUC1-DES and RUC2-DES (depending on resorcinol:urea:choline chloride molar ratio used for preparation (3.5:2:1 and 3:2:1, respectively)). The use of RC-DESs was inspired by those innovative works where the breakdown of one of the components of the DES itself (typically urea) results in the controlled delivery of an organic template to the reaction mixture.[10] In our case, RC-DES rupture and choline chloride delivery will not result from thermal decomposition (i.e., via ionothermal synthesis) but from resorcinol−formaldehyde (RF) polycondensation. Note that this sort of process, which is based on DES segregation, resembles spinodal decomposition processes that are widely used to template the texture of carbon materials.[17] Meanwhile, the use of ternary RUC-DESs was intended to imitate a recent work where urea-type ternary DESs generated porosities in metal−organic frameworks via urea incorporation into the structure and subsequent release.[11] Thus, polycondensation of RUC-DES with formaldehyde will result not only in choline chloride segregation but also in urea incorporation in the resorcinol-formaldehyde (RF) network, the release of which (by thermal treatment) could contribute to porosity generation in the resulting carbons.

Experimental Section

Preparation of Deep Eutectic Solvents (DESs). DESs were obtained by physical mixing of the individual components (resorcinol and choline chloride for RC-DES, and resorcinol, urea, and choline chloride for RUC-DES), which were thermally treated thereafter at 90 °C overnight. The resorcinol:choline chloride molar ratios were 4:1 and 3.75:1 for the preparation of RC1-DES and RC2-DES, respectively, while the resorcinol:urea:choline chloride molar ratios were 3.5:2:1 and 3:2:1 for the preparation of RUC1-DES and RUC2-DES, respectively.

Preparation of Carbons ($C_{RC\text{-}DES}$ and $C_{RUC\text{-}DES}$). Aqueous solutions composed of formaldehyde (3.1 mL, 37 wt %) and Na_2CO_3 (0.26 mL, 160 mg/mL) were added to either RC-DES or RUC-DES (2.90 mg for RC1-DES, 2.94 mg for RC2-DES, 3.68 mg for RUC1-DES, and 3.93 mg for RUC2-DES, for a 1:2 R:F molar ratio) and stirred for 30 min. Aliquots of the resulting homogeneous solution (1.5 mL) were thermally treated (first at 60 °C for 6 h and then at 90 °C for 4 days) in closed containers (to avoid evaporation). The resulting RF gels were washed before being thermally treated 4 h at 210 °C, followed by another 4 h at 800 °C (the heating ramp was 1.0 °C/min) under a nitrogen atmosphere.

Sample Characterization. DESs were studied by ^{1}H NMR spectroscopy using a Bruker spectrometer DRX-500. DESs were placed in capillary tubes, using deuterated chloroform ($CDCl_3$) as an external reference (the deuterium signal was used for locking and shimming the sample). Fourier transform infrared (FTIR) spectroscopy of the RF gels was performed in a FTIR spectrometer (Bruker Model IFS60v). Differential scanning calorimetry (DSC) was performed with a TA Instruments Model DSC Q-100 system, under a nitrogen atmosphere. The samples were run in an aluminum pan in a sealed furnace, stabilized for 30 min at 50 °C, and then cooled to −90 °C before heating at rates of 1 and 10 °C/min. The melting point (T_m) of the RC-DES samples was obtained when samples were stabilized overnight at 4 °C, rather than for 30 min at 50 °C. Raman spectra were recorded using a Renishaw InVia apparatus upon irradiation at 514 nm (100% laser power, 16 mW power, 10 accumulations, and an exposure time of 10 s). The viscosity of the DESs was measured with a Brookfield Digital Rheometer DV-III+ at 22 °C. Solid-state ^{13}C-CPMAS−NMR spectra of the RF gels were obtained using a Bruker Model AV-400-WB spectrometer, by applying a standard cross-polarization

(7) (a) Lukens, W. W.; Stucky, G. D. *Chem. Mater.* **2002**, *14*, 1665–1670. (b) Wang, Z.; Li, F.; Ergang, N. S.; Stein, A. *Chem. Mater.* **2006**, *18*, 5543–5553. (c) Liu, H.-J.; Wang, X.-M.; Cui, W.-J.; Dou, Y.-Q.; Zhao, D.-Y.; Xia, Y.-Y. *J. Mater. Chem.* **2010**, *20*, 4223.
(8) (a) Sheldon, R. *Chem. Commun.* **2001**, 2399–2407. (b) Huddleston, J. G.; Willauer, H. D.; Swatloski, R. P.; Visser, A. E.; Rogers, R. D. *Chem. Commun.* **1998**, 1765–1766. (c) Adams, C. J.; Earle, M. J.; Roberts, G.; Seddon, K. R. *Chem. Commun.* **1998**, 2097–2098.
(9) Abbott, A. P.; Capper, G.; Davies, D. L.; Rasheed, R. K.; Tambyrajah, V. *Chem. Commun.* **2003**, 70–71.
(10) (a) Abbott, A. P.; Capper, G.; Davies, D. L.; Rasheed, R. K. *Chem.−Eur. J.* **2004**, *10*, 3769–3774. (b) Fukaya, Y.; Iizuka, Y.; Sekikawa, K.; Ohno, H. *Green Chem.* **2007**, *9*, 1155–1157. (c) Parnham, E. R.; Drylie, E. A.; Wheatley, P. S.; Slawin, A. M. Z.; Morris, R. E. *Angew. Chem., Int. Ed.* **2006**, *45*, 4962–4966.
(11) (a) Cooper, E. R.; Andrews, C. D.; Wheatley, P. S.; Webb, P. B.; Wormald, P.; Morris, R. E. *Nature* **2004**, *430*, 1012. (b) Parnham, E. R.; Drylie, E. A.; Wheatley, P. S.; Slawin, A. M. Z.; Morris, R. E. *Angew. Chem.* **2006**, *118*, 5084–5088.
(12) Zhang, J.; Wu, T.; Chen, S.; Feng, P.; Bu, X. *Angew. Chem.* **2009**, *48*, 3486–3490.
(13) Xu, L.; Yan, S.; Choi, E.-Y.; Lee, J. Y.; Kwon, Y.-U. *Chem. Commun.* **2009**, 3431–3433.
(14) (a) Lin, Z.; Wragg, D. S.; Morris, R. E. *Chem. Commun.* **2006**, 2021–2023. (b) Jin, K.; Huang, X.; Pang, L.; Li, J.; Appel, A.; Wherland, S. *Chem. Commun.* **2002**, 2872–2873. (c) Dybtsev, D. N.; Chun, H.; Kim, K. *Chem. Commun.* **2004**, 1594–1595.
(15) Gutierrez, M. C.; Rubio, F.; del Monte, F. *Chem. Mater.* **2010**, *22*, 2711–2719.
(16) (a) Liang, C.; Dai, S.; Guiochon, G. *Anal. Chem.* **2003**, *75*, 4904–4912. (b) Lee, J. S.; Wang, X.; Luo, H.; Dai, S. *Avd. Mater.* **2010**, *22*, 1004–1007. (c) Paraknowitsch, J. P.; Zhang, J.; Su, D.; Thomas, A.; Antonietti, M. *Adv. Mater.* **2010**, *22*, 87–92.
(17) Liang, C.; Dai, S. *Chem. Mater.* **2009**, *21*, 2115–2124.

pulse sequence. The morphology of the different samples was studied via scanning electron microscopy (SEM), using a FE-SEM Nova Model NanoSEM 230 system and via transmission electron microscopy (TEM), using a JEOL-2000 system operating at 200 keV. Nitrogen adsorption/desorption isotherms were conducted using an Omnisorp-100 (Coulter) system on samples thermally treated overnight (RF gels at 90 °C and carbons at 250 °C) prior to nitrogen gas adsorption. Brunauer−Emmett−Teller (BET) theory and the Barrett−Joyner−Halenda (BJH) method (based on the desorption branches of the isotherms) were used to calculate the specific surface areas (S_{BET}) and pore size distributions, respectively. The microporous specific surface area (S_{mic}) and external specific surface area (S_{ext}) were calculated using the *t*-plot (see Figure S1 and Table S1 in the Supporting Information).[18] Mesopore diameters were also calculated from mercury porosimetry that was performed in a Micromeritics Autopore II 9220 system.

Results and Discussion

The formation of RC-DESs and RUC-DESs (following the process described above) was easily visualized by the liquid nature of the mixtures at room temperature (Figure 1) The melting point (T_m) of RC-DESs and RUC-DESs (from DSC scans) ranged from 68 °C to 87 °C (see Figure 1 and Table 1).[19] Note that RC-DESs display a melting point only under certain circumstances (RC-DESs are history-dependent) and never display a devitrification temperature (T_c), which reveals the difficulties of RC-DESs to crystallize upon heating. The viscosity of RUC-DESs is higher than that of RC-DESs, which corresponds with DESs having higher glass transition temperatures (T_g).[20] Interestingly, the participation of urea in the ternary complex turned the resulting RUC-DESs a blue color.[21] The formation of resorcinol−choline chloride complexes in RC-DESs and of resorcinol−urea-choline chloride complexes in RUC-DESs was also confirmed by the upfield chemical shift of the signals ascribed to both resorcinol and choline chloride in the ^{1}H NMR spectra of the mixtures (see Figure 1 and Tables S2 and S3).[22]

Carbon preparation from RC-DESs and RUC-DESs was performed using a procedure similar to that typically followed for bare resorcinol under aqueous conditions. ^{1}H NMR spectroscopy confirmed that partial DES dilution with formaldehyde and Na_2CO_3 aqueous solutions (DES concentrations in the range of 56−63 wt %; see Experimental Section) allowed several hydroxyl groups of resorcinol that were forming the DESs to be available for polycondensation reactions (see Figure 1, as well as Figure S2 and Tables S2 and S3 in the Supporting Information). This is an important issue, because the presence of water influences the structure of DESs. Thus, depending on water concentration, one can have a situation where either water molecules are solvated by DES or the opposite. In this latter case (that is, DES molecules solvated by water), we would not have a DES any longer, but rather a simple dissolution of the individual molecules of DES in water. However, partial rupture of DES (for instance, because of the presence of water at a

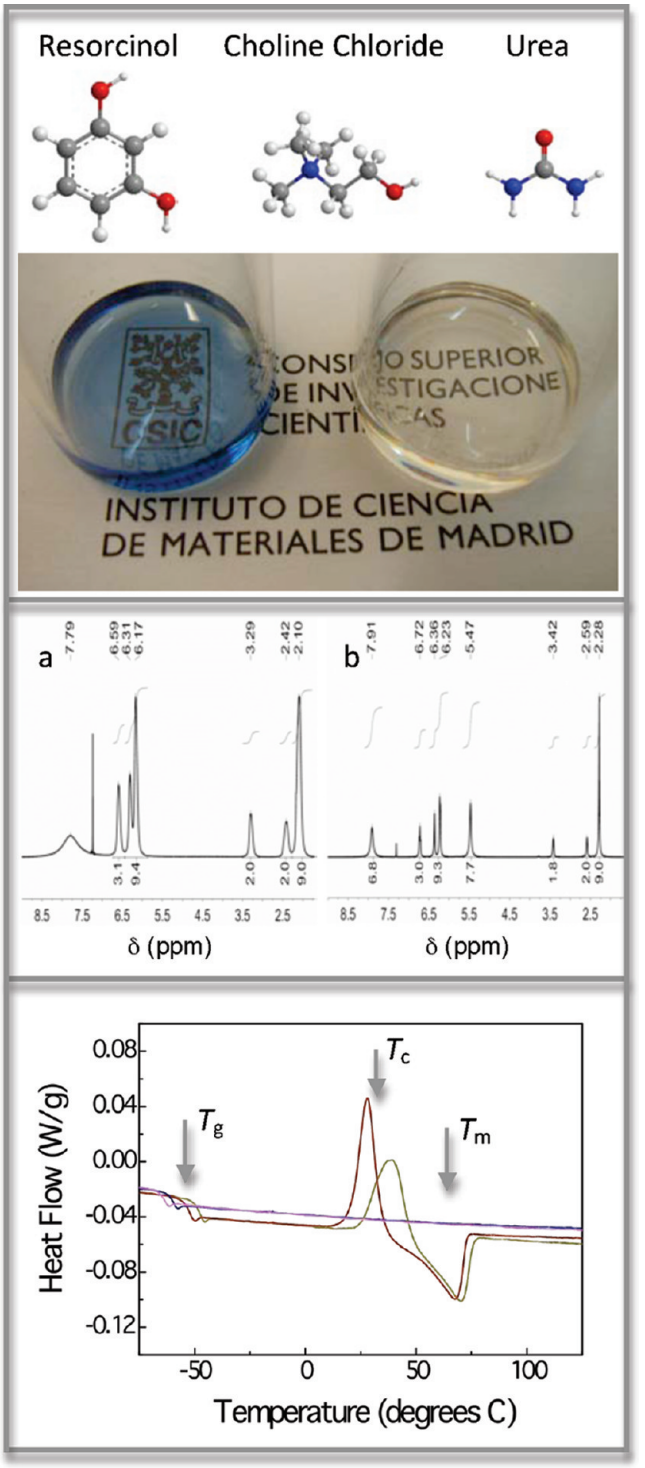

Figure 1. (Top panel) Molecules forming the DESs and picture of two of them; RUC1-DES (left) and RC1-DES (right). (Middle panel) ^{1}H NMR spectra of (a) RC2-DES and (b) RUC2-DES. (Bottom panel) DSC traces taken at a rate of 1 °C/min of RC1 (blue line), RC2 (magenta line), RUC1 (red line), and RUC2 (dark yellow line). RC1 and RC2 only displayed a glass-transition temperature (T_g), whereas RUC1 and RUC2 displayed a melting point (T_m), a crystallization temperature (T_c), and a glass-transition temperature (T_g).

(18) Lippens, B. C.; de Boer, J. H. *J. Catal.* **1965**, *4*, 319.
(19) Greaves, T. L.; Weerawardena, A.; Fong, C.; Krodkiewska, I.; Drummond, C. J. *J. Phys. Chem. B* **2006**, *110*, 22479–22487.
(20) Xu, W.; Cooper, E. I.; Angell, C. A. *J. Phys. Chem. B* **2003**, *107*, 6170.
(21) Pizzi, A.; Pasch, H.; Simon, C.; Rode, K. *J. Appl. Polym. Sci.* **2004**, *92*, 2665–2674.
(22) (a) Gutierrez, M. C.; Ferrer, M. L.; Mateo, C. R.; del Monte, F. *Langmuir* **2009**, *25*, 5509–5515. (b) Gutierrez, M. C.; Ferrer, M. L.; Yuste, L.; Rojo, F.; del Monte, F. *Angew. Chem., Int. Ed.* **2010**, *49*, 2158–2162.

Table 1. Viscosities (η), Glass Transition Temperature (T_g), Devitrification Temperature (T_c) and Melting Point (T_m) of RC-DESs and RUC-DESs[a]

	η (cP)	T_g (°C)	T_c (°C)	T_m (°C)
RC1-DES	1883	−60.0[b]	[c]	87.0[d]
RC2-DES	1813	−64.0[b]	[c]	86.0[d]
RUC1-DES	2348	−48.5[b]	39[b]	70.5[b]
RUC2-DES	2440	−53.0[b]	28[b]	68.0[b]

[a] T_g values were determined from Figure 1 at the point where the extrapolated lines from the baseline and the glass transition "cliff" intersected. T_c and T_m values were determined from Figure 1 at the exothermic peak and the endothermic peak, respectively. [b] Traces obtained at a rate of 1 °C/min. [c] RC1 and RC2 did not display T_c transitions under any of the experimental conditions used in this work. [d] Traces taken at 10 °C/min. RC1 and RC2 were stored at 4 °C overnight (hence, in its solid form) prior DSC analysis.

determined weight percentage) was actually crucial to carry out the polycondensation of one of the DES components (that is, resorcinol). Otherwise, polycondensation was impeded because of the unavailability of resorcinol when this is forming the DES. Under these circumstances, we considered it necessary to determine the threshold water concentration that retains a major fraction of the supramolecular complexes which characterize DESs but allows some resorcinol to be available for polycondensation. As described in detail in some of our previous works, ^{1}H NMR spectroscopy is an excellent tool to study whether supramolecular complexes remains in partially diluted DESs.[15,22] The dilutions used for polycondensation were 56 wt % for RC1-DES, 57 wt % for RC1-DES, 62 wt % for RUC1-DES, and 63 wt % for RUC1-DES, so we decided to study D_2O solutions of these samples (e.g., RC1-DES56, RC2-DES57, RUC1-DES62, and RUC2-DES63). We also studied the D_2O solutions RC-DES and RUC-DES that had DES contents of 100 wt % (e.g., nondiluted), 85 wt %, and 10 wt %. The spectra of nondiluted samples (see RC1-DES, RC2-DES, RUC1-DES, and RUC2-DES in Figure 1, and Tables S2 and S3 in the Supporting Information) revealed that the characteristic signals of both choline chloride (mostly those assigned to CH_3 and CH_2 in position 1) and resorcinol (mostly those assigned to CH in positions 2, 4, and 6) protons were shifted upfield (up to 0.9 ppm for chloline chloride), compared to those obtained for resorcinol or choline chloride in separate D_2O solutions (see samples R and C in Tables S2 and S3 in the Supporting Information). Thus, upfield chemical shifts were indicative of the formation of ion−hydrogen-bond-donor supramolecular complexes, which characterize DESs. The spectra of diluted samples exhibited a progressive downfield shift of the signals as dilution increases. Actually, the chemical shifts found in DES10 samples are similar to those obtained for single resorcinol or choline chloride in separate D_2O solutions, which reveals the total rupture of ion−hydrogen-bond-donor supramolecular complexes that characterize DESs for 10 wt % dilution. The chemical shifts found in those dilutions used for polycondensation reactions samples (e.g., RC1-DES56, RC2-DES57, RUC1-DES62, and RUC2-DES63 in Figure S2) were more similar to those obtained for DES and DES85 than to those obtained for DES10 (see data in Tables S2 and S3 in the Supporting Information). Further corroborating this issue is the upfield shift of the HDO signal (resulting from proton interchange with D_2O) in the spectra of RC-DES and RUC-DES samples that had DES contents of 85 wt % and ca. 60 wt %, as a consequence of the formation of weak hydrogen-bonding structures in HDO (that is, HDO is solvated by halide-ion−hydrogen-bond-donor supramolecular complexes). Meanwhile, the downfield shift of the HDO signal in the spectra of DES10 is similar to that found in the spectra of both single choline chloride and resorcinol, which indicates that HDO is solvating the individual molecules of choline chloride and resorcinol that result from DES rupture.

These features revealed that, for ca. 60 wt % dilutions (that is, the dilution used for polycondensation), most of the ion−hydrogen-bond-donor supramolecular complexes that characterize DESs remain, while some of them are broken, the rupture of which provided enough resorcinol to start the polycondensation reaction. Further RF polycondensation resulted in the segregation of the second component of DES (e.g., choline chloride) which, acting as template agent, promoted the formation of a bicontinuous porous network built of highly cross-linked clusters that aggregated and assembled into a stiff, interconnected structure (see SEM micrographs in Figure 2, top panel). Nitrogen adsorption/desorption measurements provided surface areas (S_{BET}) of 266 m^2/g for $RF_{RC1\text{-}DES}$ gels, 270 m^2/g for $RF_{RC2\text{-}DES}$ gels, 66 m^2/g for $RF_{RUC1\text{-}DES}$ gels, and 60 m^2/g for $RF_{RUC2\text{-}DES}$ gels (see Figure S3 in the Supporting Information). However, the accuracy of these data should be taken with caution, because of the low temperature used to degasify the RF gels.

The occurrence of choline chloride segregation during RF polycondensation was investigated by washing the RF gels twice with an abundance of water (ca. 35 mL) for clearance of noncondensed reagents. The ^{1}H NMR spectra of the residue obtained after washing $RF_{RC\text{-}DES}$ gels corresponded to choline chloride (see Figure S4 in the Supporting Information) and its weight revealed the amount of full choline chloride recovered. Meanwhile, the ^{1}H NMR spectra of the residue obtained after washing $RF_{RUC\text{-}DES}$ gels corresponded to choline chloride and urea (see Figure S4 in the Supporting Information); but, while the recovery of choline chloride was also complete, urea recovery was only partial and indicated the participation of urea in condensation reactions and its incorporation into the RF network.

FTIR and solid ^{13}C NMR spectroscopy of $RF_{RC\text{-}DES}$ and $RF_{RUC\text{-}DES}$ gels (after washing and freeze-drying) corroborated these findings. Thus, the intensity of bands assigned to methylene (CH_2 groups at ca. 2938 and 1479 cm^{-1}) and methylene ether groups (C−O benzyl ether groups at 1230 and 1100 cm^{-1}) in the FTIR spectra were indicative of a significant number of linkages between resorcinol rings (Figure 3).[23] In solid ^{13}C NMR spectra, the integration of the signal at 152 ppm (assigned to

(23) Yangfei, C.; Zhiqin, C.; Shaoyi, X.; Hongbo, L. *Thermochim. Acta* **2008**, *476*, 39–43.

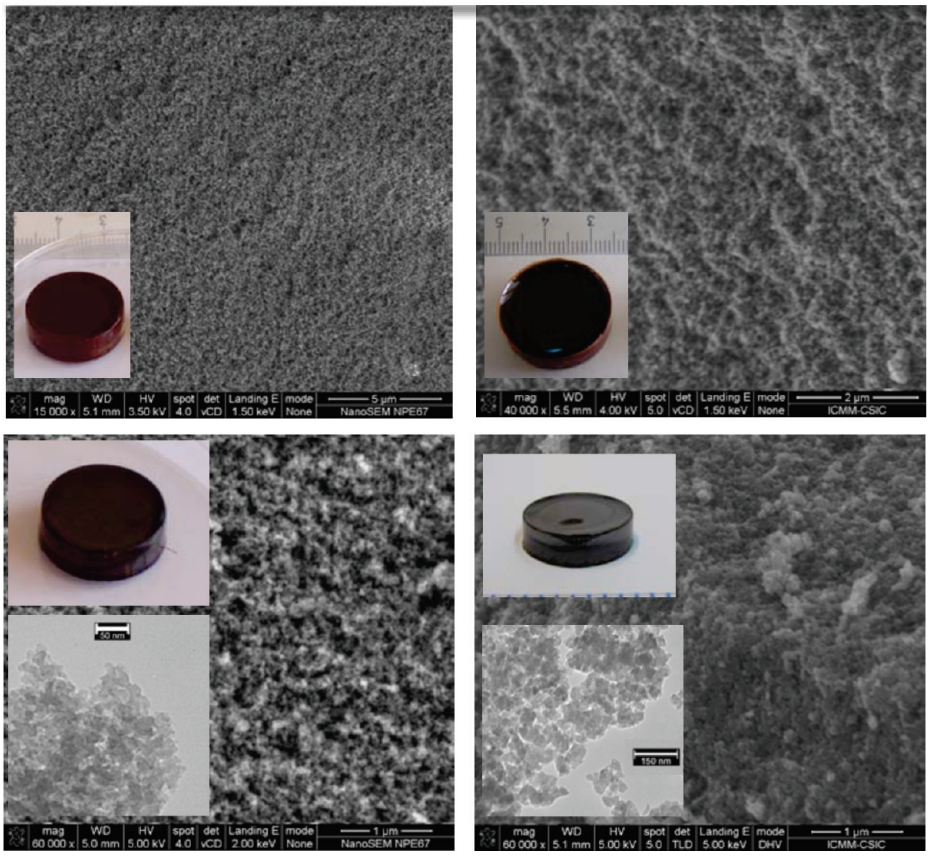

Figure 2. (Top panel) SEM micrographs of $RF_{RC1\text{-}DES}$ (left, bar = 5 μm) and $RF_{RUC1\text{-}DES}$ (right, bar = 2 μm) gels; insets show images of the monolithic RF gels. (Bottom panel) SEM micrographs of $C_{RC1\text{-}DES}$ (left, bar = 1 μm) and $C_{RUC1\text{-}DES}$ (right, bar = 1 μm) monoliths; insets show TEM micrographs of $C_{RC1\text{-}DES}$ (left, bar = 50 nm) and $C_{RUC1\text{-}DES}$ (right, bar = 150 nm) and a picture of the respective monolithic carbons.

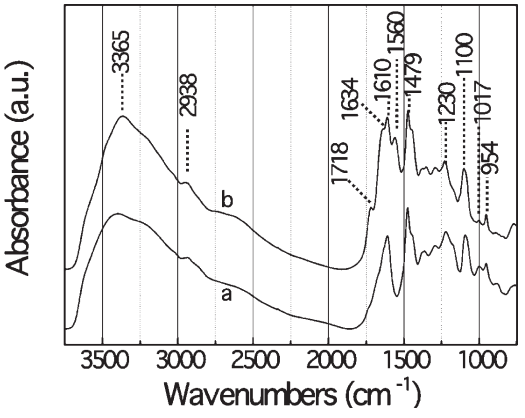

Figure 3. Fourier transform infrared (FTIR) spectra of (a) $RF_{RC1\text{-}DES}$ and (b) $RF_{RUC1\text{-}DES}$ gels.

aromatic phenolic carbon) versus the sum of the signals at 20−40 ppm plus that at 59 ppm (assigned to methylene and methylene ether groups, respectively) also revealed the efficient chemical make up of both $RF_{RC\text{-}DES}$ and $RF_{RUC\text{-}DES}$ gels (see Figure 4).[24] With regard to the eventual incorporation of urea into the RF gels, the appearance of the signal at 161 ppm in the solid ^{13}C NMR spectrum, as well as the band at 1634 cm^{-1} in the FTIR spectrum of $RF_{RUC\text{-}DES}$ gels (both ascribed to carbonyl groups of substituted urea[25]), confirmed this issue. Actually, the relative intensity of the band at 1017 cm^{-1} (ascribed to 1,2- and 1,4-substituted aromatic rings) versus that at 954 cm^{-1} (ascribed to C−O stretch of resorcinol) in the FTIR spectrum of $RF_{RC\text{-}DES}$ gels was higher than in that of $RF_{RUC\text{-}DES}$ gels, as a consequence of the incorporation of urea into the linear backbone of the $RF_{RUC\text{-}DES}$ gels. Thermogravimetry (TG) analysis of $RF_{RC\text{-}DES}$ and $RF_{RUC\text{-}DES}$ gels allowed the estimation of the urea incorporation into the $RF_{RUC\text{-}DES}$ network. The thermal decomposition of RC-DESs and RUC-DESs was quite similar and occurred within the temperature range of 150−300 °C (see Figure 5, top panel). However, the TG curves of the $RF_{RUC\text{-}DES}$ and $RF_{RC\text{-}DES}$ differed by ca. 8% (see Figure 5, bottom panel). Interestingly, discrepancies in the weight loss pattern were localized within the 200−300 °C range, which is the temperature at which urea and condensed urea byproduct (e.g., biuret and cyanuric acid) have been reported to decompose.[26]

Carbonization of washed $RF_{RC\text{-}DES}$ and $RF_{RUC\text{-}DES}$ gels was accomplished at 800 °C in N_2 atmosphere with carbon conversions of ~80%. The graphitic character (see X-ray diffraction (XRD) and Raman spectra in Figure S5 of the Supporting Information) and the oxygen contents

(24) Mulik, S.; Sotiriou-Leventis, C.; Leventis, N. *Chem. Mater.* **2007**, *19*, 6138–6144.

(25) Mulik, S.; Sotiriou-Leventis, C.; Leventis, N. *Chem. Mater.* **2008**, *20*, 6985–6997.

(26) Schaber, P. M.; Colson, J.; Higgins, S.; Thielen, D.; Anspach, B.; Brauer, J. *Thermochim. Acta* **2004**, *424*, 131–142.

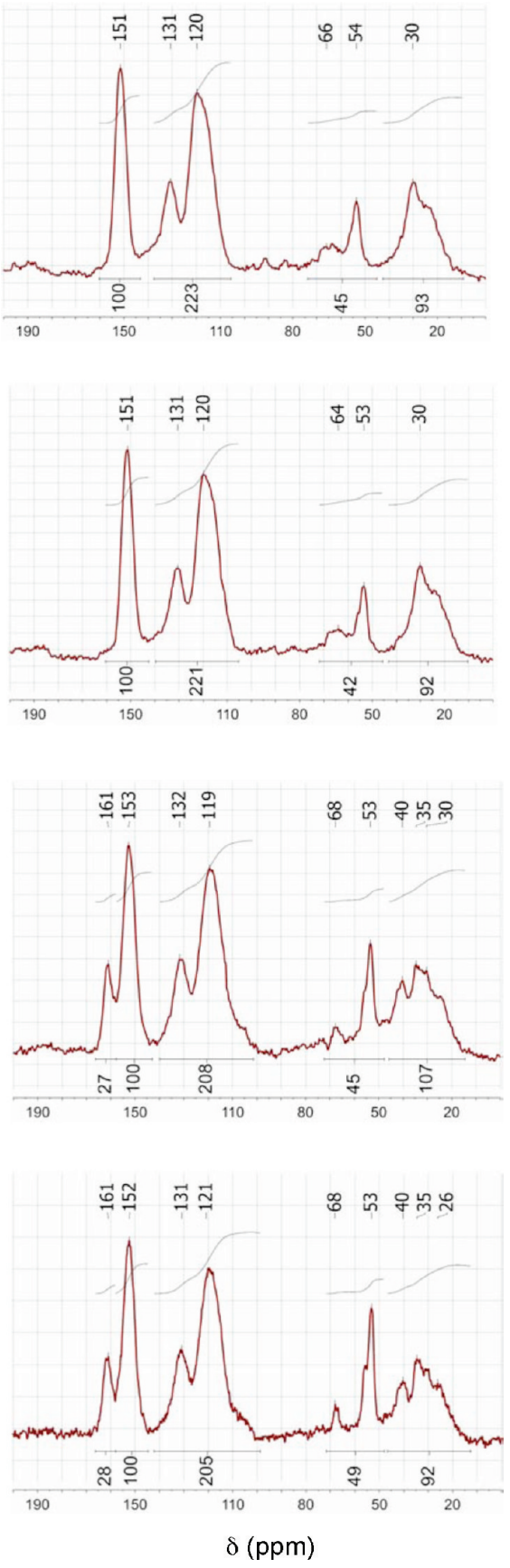

Figure 4. Solid ^{13}C NMR spectra of (from top to bottom) $RF_{RC1\text{-}DES}$, $RF_{RC2\text{-}DES}$, $RF_{RUC1\text{-}DES}$, and $RF_{RUC2\text{-}DES}$ gels.

(ca. 5%, see EDX in Figure S6 of the Supporting Information) of the resulting monolithic carbons were in the

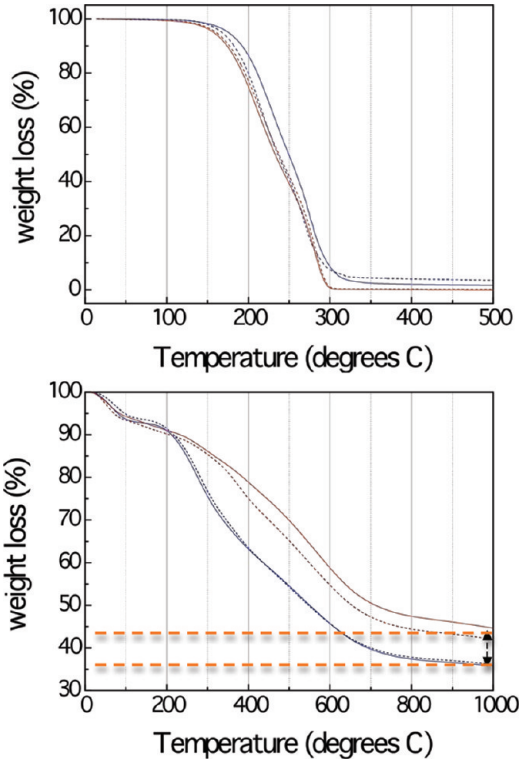

Figure 5. (Top panel) TG analysis of RC1-DES (red solid line), RC2-DES (red dash line), RUC1-DES (blue solid line), and RUC2-DES (blue dash line). (Bottom panel) Thermogravimtry (TG) analysis of $RF_{RC1\text{-}DES}$ (red solid line), $RF_{RC2\text{-}DES}$ (red dash line), $RF_{RUC1\text{-}DES}$ (blue solid line), and $RF_{RUC2\text{-}DES}$ (blue dash line) gels.

Table 2. Summary of the Data Obtained from Nitrogen Adsorption/Desorption Isotherms and Mercury Porosimetry for $C_{RC1\text{-}DES}$, $C_{RC2\text{-}DES}$, $C_{RUC1\text{-}DES}$, and $C_{RUC2\text{-}DES}$

	$C_{RC1\text{-}DES}$	$C_{RC2\text{-}DES}$	$C_{RUC1\text{-}DES}$	$C_{RUC2\text{-}DES}$
S_{BET} (m^2/g)[a]	518	612	576	455
S_{mic} (m^2/g)[b]	254	296	333	267
S_{ext} (m^2/g)[b]	264	316	243	188
S_{mic} (%)[b]	49	48	58	59
V_{total} (cm^3/g)[b]	0.55	0.61	0.61	0.57
V_{mic} (cm^3/g)[b]	0.13	0.15	0.18	0.14
mean pore diameter (nm)				
BJH[c]	10	10	23	23
Hg porosimetry[d]	9	8	21	21
bulk density (g/cm^3)[d]	1.02	1.08	0.99	0.99
skeletal density (g/cm^3)[d]	1.37	1.36	1.47	1.36
porosity (%)[d]	25.7	20.4	32.6	26.7

[a] Obtained from nitrogen adsorption/desorption isotherms. [b] Obtained from t-plot. [c] Obtained from BJH analysis of the data. [d] Obtained from mercury porosimetry.

ranges of those typically found in carbons obtained from RF gels synthesized under aqueous conditions. Both $C_{RC\text{-}DES}$ and $C_{RUC\text{-}DES}$ were composed of sintered carbon colloids, which is the typical morphology of carbons obtained via sol−gel processes based on resorcinol−formaldehyde polycondensation (see Figure 2, bottom panel). TEM micrographs revealed that the sizes of the carbon colloids strongly differ from $C_{RC\text{-}DES}$ to $C_{RUC\text{-}DES}$ (ca. 14 and 35 nm, respectively). Nitrogen adsorption/desorption measurements provided similar surface areas (S_{BET}) for $C_{RC\text{-}DES}$ and $C_{RUC\text{-}DES}$ (see Table 2, Figure 6, and Figure S7 in the Supporting Information): 518 m^2/g for $C_{RC1\text{-}DES}$, 612 m^2/g

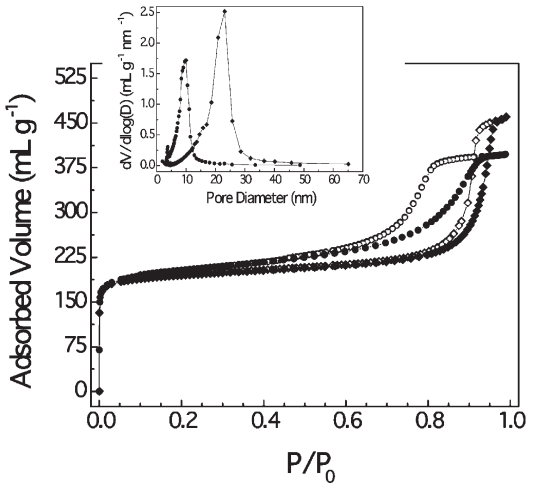

Figure 6. Adsorption (solid symbols) and desorption (open symbols) nitrogen isotherms of $C_{RC2\text{-}DES}$ (circles) and $C_{RUC1\text{-}DES}$ (diamonds). Inset shows pore size distributions of $C_{RC2\text{-}DES}$ (circles) and $C_{RUC1\text{-}DES}$ (diamonds).

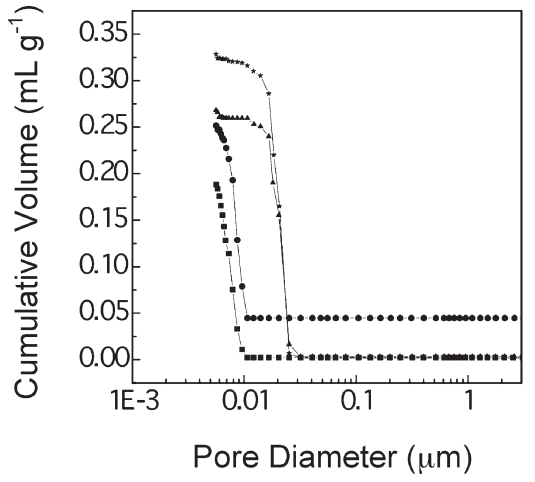

Figure 7. Plot of cumulative volume versus pore diameter for $C_{RC1\text{-}DES}$ (circles), $C_{RC2\text{-}DES}$ (squares), $C_{RUC1\text{-}DES}$ (stars), and $C_{RUC2\text{-}DES}$ (triangles) obtained from mercury porosimetry measurements. Pore diameters (e.g., ca. 10 nm for $C_{RC1\text{-}DES}$ and $C_{RC2\text{-}DES}$, and ca. 23 nm for $C_{RUC1\text{-}DES}$ and $C_{RUC2\text{-}DES}$) were consistent with those obtained from application of the BJH method to nitrogen adsorption−desorption isotherms.

for $C_{RC2\text{-}DES}$, 576 m^2/g for $C_{RUC1\text{-}DES}$, and 455 m^2/g for $C_{RUC2\text{-}DES}$. Interestingly, ca. 50% of surface area in $C_{RC\text{-}DES}$ and 60% in $C_{RUC\text{-}DES}$ corresponded to micropores (S_{mic} in Table 2, calculated from the *t*-plot), whereas the mesopore diameter (see BJH plots in the inset of Figure 6 and Figure S7 in the Supporting Information) differed, depending on the use of urea as a component of the starting DES with pore diameters of ca. 23 nm for $C_{RUC\text{-}DES}$ and ca. 10 nm for $C_{RC\text{-}DES}$ (also confirmed by mercury porosimetry; see Table 2 and Figure 7). The mesopore diameter enhancement found for $C_{RUC\text{-}DES}$ must be related to the use of urea-based DESs, its incorporation into the RF gel, and its subsequent release during carbonization. Actually, the nitrogen content of $RF_{RUC\text{-}DES}$ gels (observed by ^1H NMR and FTIR spectroscopy) vanished in $C_{RUC\text{-}DES}$ (nitrogen was not observed by SEM-EDX analysis, as observed in Figure S6 in the Supporting Information), opposite to previous works using nitrogen-containing precursors.[27] The lack of texture observed in RF gels prepared in the absence of choline chloride (see Figure S8 in the Supporting Information) confirmed the capital role played by DESs in pores generation.

Conclusions

We have described the synthesis of deep eutectic solvents (DESs) based on resorcinol, the use of which, both as carbonaceous precursors and template agents, allowed the preparation of hierarchical porous (bimodal, with micropores and mesopores) carbon monoliths via formaldehyde polycondensation and subsequent carbonization. The performance of resorcinol-based DESs as carbonaceous precursors was remarkable, with carbon conversions of ~80%. Moreover, the template effect of DESs was reflected in the achievement of hierarchical porous carbon monoliths with pore surface areas up to 600 m^2/g and narrow mesopore diameter distributions. The mechanism governing mesopores formation is based on a spinodal-decomposition-like process via resorcinol polycondensation and subsequent segregation of the resorcinol counterpart that is forming the DES (choline chloride in RC-DESs, and choline chloride and urea in RUC-DESs). Template delivery via DESs decomposition is actually one of the most interesting structure-directing processes used to obtain zeolites.[11] Interestingly, the use of resorcinol-based DESs that also contained urea resulted in the formation of larger mesopores (ca. 23 nm for containing-urea DESs versus ca. 10 nm for noncontaining-urea ones), as a consequence of the incorporation of urea into the RF network, the release of which, during carbonization, contributed to pore diameter enhancement. This latter approach, where the components of urea-type ternary DESs can generate porosities via either segregation or incorporation into the network, also resembles the recently reported synthesis of metal−organic frameworks that are characterized by their versatility in the creation of different pore morphologies.[12] We consider that the different uses of DESs as structure-directing agents described herein (e.g., template segregation and template incorporation into the network) open the path to new types of carbon chemistry that may not be accessible in either ionic liquids (ILs) or molecular solvent agents.

Acknowledgment. This work was supported by MICINN (MAT2009-10214 and PET2008-0168-01). D.C. acknowledges MICINN for a JdlC research contract.

Supporting Information Available: Supporting Information for this article includes ^1H NMR spectra of D_2O dilutions of DESs, nitrogen adsorption isotherms of RF gels and XRD and Raman spectra, EDX analysis, nitrogen adsorption isotherms and t-plots of carbons. This material is available free of charge via the Internet at http://pubs.acs.org.

(27) Gorgulhoa, H. F.; Gonçalves, F.; Pereira, M. F. R.; Figueiredo, J. L. *Carbon* **2009**, *47*, 2032–2039.